Velocity distributions in dilute granular systems

J. S. van Zon[1,2,*] and F. C. MacKintosh[1,2,†]
[1]*Division of Physics and Astronomy, Vrije Universiteit, 1081 HV Amsterdam, The Netherlands*
[2]*Kavli Institute for Theoretical Physics, University of California, Santa Barbara, California 93106, USA*
(Received 30 October 2003; revised manuscript received 6 August 2004; published 11 November 2005)

We investigate the idea that velocity distributions in granular gases are determined mainly by η, the coefficient of restitution and q, which measures the relative importance of heating (or energy input) to collisions. To this end, we study by numerical simulation the properties of inelastic gases as functions of η, concentration ϕ, and particle number N with various heating mechanisms. For a wide range of parameters, we find Gaussian velocity distributions for uniform heating and non-Gaussian velocity distributions for boundary heating. Comparison between these results and velocity distributions obtained by other heating mechanisms and for a simple model of a granular gas without spatial degrees of freedom, shows that uniform and boundary heating can be understood as different limits of q, with $q \gg 1$ and $q \lesssim 1$ respectively. We review the literature for evidence of the role of q in the recent experiments.

DOI: 10.1103/PhysRevE.72.051301 PACS number(s): 81.05.Rm, 05.20.Dd, 83.10.Pp

I. INTRODUCTION

Granular materials consist of macroscopic particles, such as sand grains or metal beads, but can, nevertheless, exhibit behavior reminiscent of the conventional phases of matter. A layer of sand, for instance, can flow down an incline, much like a liquid. Likewise, dilute granular systems are frequently called gases because of many similarities to molecular gases. In contrast with molecular gases, however, granular *gases* are intrinsically dissipative and out of equilibrium. In fact, such systems have been extensively studied both experimentally and theoretically, in large part as simple model systems exhibiting nonequilibrium and dissipative behavior. Unlike molecular gases, the collisions in a granular gas are inelastic, making it necessary to drive them in order to maintain a gaslike steady state. Otherwise, *inelastic collapse* can occur, in which all motion ceases after only a finite time [1,2]. In some simulations [3–6] and in most analytic theories [7–9], this driving or *heating* is done uniformly throughout the container (*uniform heating*), with all the particles in the gas being driven independently by a white-noise source. In experiments, on the other hand, the granular gas is driven by shaking or vibrating the walls of the container. With this *boundary heating*, energy is inserted in a spatially inhomogeneous way [10–14], often resulting in gradients in density and mean kinetic energy [14,15]. Uniformly heated granular gases can also show significant deviations from equilibrium gases, e.g., in density correlations [3].

One of the most basic properties of ordinary gases is the velocity distribution, which is a Maxwell-Boltzmann or Gaussian distribution. Dilute granular systems, however, deviate from the Gaussian distributions that one would expect if the collisions were elastic. It has been suggested that the velocity distributions can be described by a sort-of *stretched* Gaussian, of the form $P(v)=C\exp[-\beta(v/\sigma)^{\alpha}]$, where $\sigma^2=\langle v^2\rangle$ is sometimes called the granular temperature. Rouyer and Menon [10] have reported such a distribution with exponent $\alpha=1.5$ over the whole observed range of velocities, which was unaffected by changes in amplitude and frequency of driving. This same exponent is predicted for the asymptotic high velocity tail by certain kinetic theory models of granular gases [7]. However, it is shown in Ref. [10] that the experimentally observed non-Gaussian distribution is not consistent with the high velocity tail predicted by kinetic theories. Since then, experiments and simulations have observed many more, qualitatively different velocity distributions, depending on the driving mechanisms and the properties of the gas itself. As a consequence, it has remained unclear as to what extent there exists an analog to the Maxwell-Boltzmann equation in granular gases. Also, a clear physical picture of the origin of non-Gaussian velocity distributions is still lacking.

In a previous publication [16], we presented evidence that the velocity distribution in granular gases is predominantly determined by just two parameters: the coefficient of restitution η and $q=N_H/N_C$, the ratio between the average number of heatings and collisions in the gas. The first is a material parameter and describes the amount of dissipation in collisions. The latter is controlled by the mechanism of energy injection and depends sensitively on the experimental setup. Because of the dependence on q, experiments on the same granular gas could yield different velocity distributions depending on the details of driving. This can explain the seemingly inconsistent results from recent experiments. Furthermore, we showed that the velocity distributions for uniform and boundary heating are very different. For uniform heating, the velocity distributions remain close to Gaussian. For boundary heating, a family of distributions is observed, with different exponents for the high velocity tail. Finally, we found no evidence for a universal velocity distribution with exponent $\alpha=1.5$.

In this manuscript, we systematically study the velocity distribution as a function of the coefficient of restitution η, the area density ϕ, and the particle number N, both for uni-

*Electronic address: jvzon@nat.vu.nl
†Electronic address: fcm@nat.vu.nl

form and boundary heating. For boundary heating, we study the velocity distribution as a function of the gradient in density and granular temperature that develops in the container. We also examine the velocity distribution for different heating mechanisms and for a model without spatial degrees of freedom. Taken together, these results strengthen the picture in Ref. [16] that the velocity distribution is mainly determined by just two parameters η and q, as defined above. We also review the evidence of the role of q in recent experiments.

II. NUMERICAL SIMULATION

We use an event-driven algorithm to simulate N particles of radius a moving in a two-dimensional box. Particles gain energy by heating and lose energy through inelastic collisions. When two particles i and j collide their final velocities depend on their initial velocities in the following way:

$$\mathbf{v}_i' = \mathbf{v}_i - \frac{1+\eta}{2}(\mathbf{v}_i \cdot \hat{\mathbf{r}}_{ij} - \mathbf{v}_j \cdot \hat{\mathbf{r}}_{ij})\hat{\mathbf{r}}_{ij}, \tag{1}$$

where $0 \leqslant \eta < 1$ is the coefficient of restitution and $\hat{\mathbf{r}}_{ij}$ is the unit vector connecting the centers of particles i and j.

For uniform heating we adapted a one-dimensional algorithm described in [3]. When heating uniformly, each individual particle is heated by adding a random amount to the velocity of each particle during a time step Δt:

$$\mathbf{v}_i(t+\Delta t) = \mathbf{v}_i + \sqrt{h\Delta t}\mathbf{f}(t), \tag{2}$$

where $\mathbf{f}(t)$ is a random vector whose components are uniformly distributed between $-\frac{1}{2}$ and $\frac{1}{2}$ and h is proportional to the heating rate. After heating the system is transferred to the center-of-mass frame. Particles move in a box with periodic boundary conditions to simulate bulk behavior. The time step Δt is chosen in such a way that on average the number of collisions per time step is less than 1. It should be noted that this heating mechanism is significantly different from the spatially homogeneous heating used in some experiments [17]. In the experiment all particles feel the same forcing, so the motion of the neighboring particles is strongly correlated in space and time. In uniform heating however, all particles are independently driven by a stochastic source and as a consequence correlations are very weak.

When heating through the boundaries, particles gain velocity upon collision with the boundary. For simplicity, we assume that the collision with the boundary is elastic. In that case, a collision occurs by reflecting $\mathbf{v}_\perp$, the component of the velocity perpendicular to the boundary. Heating occurs by adding a random amount of velocity to $\mathbf{v}_\perp$. Then after collision with the boundary one has

$$\mathbf{v}_i' = \mathbf{v} - 2\mathbf{v}_\perp + \sqrt{h}\mathbf{f}(t). \tag{3}$$

Particles move in a circular box. A symmetrical container has the advantage that it allows us to examine density and granular temperature gradients along a single coordinate r, the distance from the center of the box, as in the one-dimensional case [15]. This method of heating at the boundary is analogous to the technique described in [14].

We start the simulation by distributing the particles uniformly over the box. When using boundary heating, we give each particle a small, uniformly distributed velocity to enable particles to reach the boundary. Then particles are heated and we allow the system to reach a steady state before taking data. For both uniform heating and boundary heating, data are collected periodically at every time step Δt. For uniform heating, data are taken when the particles are heated, so Δt equals the time between heating events.

III. SIMULATION RESULTS: CLUSTERING

Dense clusters of particles occur for a wide range of parameters when heating through the boundary, but are absent for uniform heating [16]. This occurs as particles are compressed in the center of the box by the pressure of particles moving in from the boundary. As the cluster grows in size, it can no longer be destroyed by the impact of high velocity particles and the cluster remains stable. Examples for increasing amounts of dissipation are shown in Fig. 1. As energy dissipation is increased, either by decreasing η or increasing the number of collisions, the gas develops a liquidlike cluster surrounded by a hot gas. For higher dissipation, the cluster grows in size and ultimately shows crystalline order, including defects and disclinations. The smaller clusters are highly dynamic and assemble and disassemble as they move around the container.

For measurements of the velocity distribution, the gas has to be in the homogeneous gas state. To avoid values of ϕ and η corresponding to the formation of clusters in our simulation, we constructed a phase diagram. We did this by counting for every particle the average number N_{6a} of neighbors with their center within a distance smaller than or equal to $6a$ from that particle. When the gas is in a hexagonal close packed state $N_{6a}=36$. We obtained the distribution $P(N_{6a})$ for different values of ϕ and η. An example for $N=350$ and $\phi=0.1$ is shown in Fig. 2.

For $\eta=0.9$ the distribution corresponds to a state with the particles uniformly distributed over the box and the peak of the distribution at the mean value $\bar{N}_{6a}=3.6$. For $\eta=0.7$ the distribution becomes bimodal, with a broad peak at high N_{6a} corresponding to the densely-packed cluster and a peak at $N_{6a}=1$ corresponding to the surrounding dilute gas. The distribution shows a continuous variation for η in between, which makes it hard to pinpoint an exact value of η for which clusters first form. Still, by looking at the shape of the distributions, it can be argued that the transition occurs somewhere between $\eta=0.75$ and $\eta=0.85$. This was repeated for different values of ϕ, which allowed us to determine a sort of phase or state diagram. Specifically, we determined the limit of a pure gaslike phase, and all results presented below were obtained in this state. Unfortunately, as the transistion from the homogenous gas state to the cluster state is very gradual, we are unable to present here an accurate phase diagram.

IV. SIMULATION RESULTS: VELOCITY DISTRIBUTIONS

The velocity distributions $P(v_x)$ for uniform heating are shown in Figs. 3 and 4. The velocity component v_x is scaled

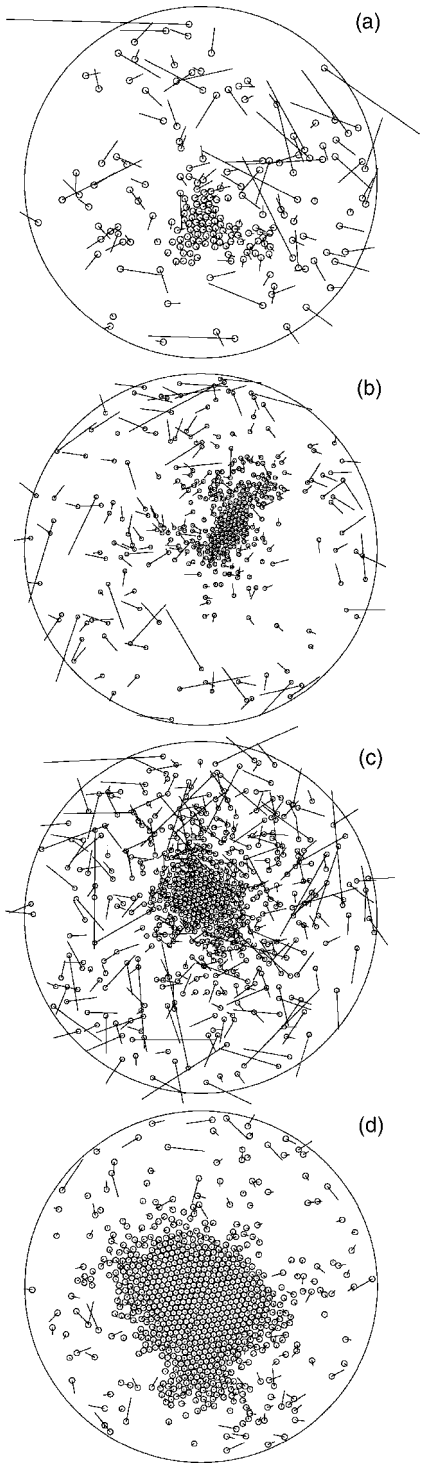

FIG. 1. Snapshots of the clustered state for (a) $N=200$, $\phi=0.06$, and $\eta=0.5$; (b) $N=400$, $\phi=0.05$ and $\eta=0.6$; (c) $N=600$, $\phi=0.1$ and $\eta=0.8$; and (d) $N=800$, $\phi=0.2$ and $\eta=0.7$. The circles indicate the current positions of the particles, while the lines show the direction and magnitude of the velocity. The smaller clusters show more liquidlike order, whereas in the bigger clusters the order is crystalline. In the latter case, the hexagonal ordering of the clusters sometimes shows defects. In (d), for instance, the cluster appears to exhibit distinct crystal-like domains.

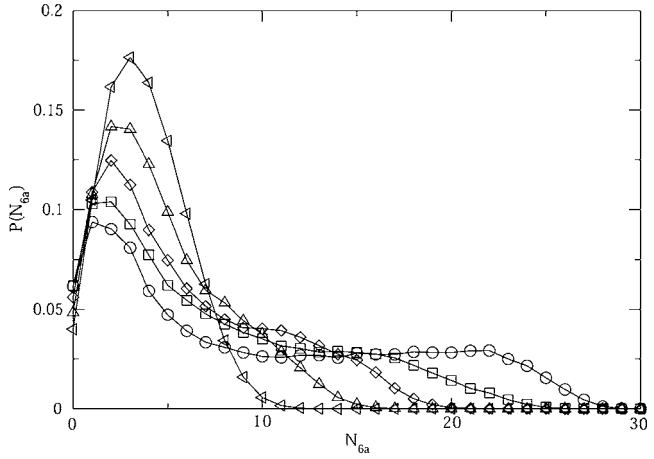

FIG. 2. Number of neighbors within a distance $6a$ of a given particle for $N=350$, $\phi=0.1$ and $\eta=0.7$ (○), 0.75 (□), 0.8 (◇), 0.85 (△), and 0.9 (◁). On average $N_{6a}=3.6$ for $\phi=0.1$.

by $\sigma_x=\langle v_x^2\rangle^{1/2}$ and the maximum of the distribution $P(v_x/\sigma_x)$ is scaled to be unity. For a broad range of the parameters ϕ and η the velocity distributions are very close to Gaussian. For $\eta=0.8$ the velocity distributions can be fitted by a distribution with $\alpha=2.0$. This decreases only slightly for $\eta=0.1$, which can be fitted by a distribution with $\alpha=1.9$. Values of α are found to be independent of ϕ. These exponents are constant over the entire observed range of velocities and we find no evidence of a velocity distribution with $\alpha=1.5$ for the range of ϕ and η we examined. This agrees with observations made before in Ref. [18].

For boundary heating the gas develops a gradient in both density and mean kinetic energy as shown in Figs. 5 and 6. Ideally, we want to measure velocity distributions in a region where the gradient is small. To this end we divided the box in five rings of width 0.2. These rings are indicated in Figs. 5 and 6. Only for values of ϕ and η close to the clustering state, does the density within a ring vary by more than 10%. The velocity distributions $P(v_x)$ for particles within the different rings are shown in Fig. 7. Figure 7(a) shows $P(v_x)$ with the velocity component v_x scaled by $\sigma_x=\langle v_x^2\rangle^{1/2}$ and the maximum of the distribution scaled to be unity. When normalized by σ_x the velocity distributions for different rings in the container have largely the same shape for smaller velocities, even though density and mean kinetic energy vary considerably between these rings. This is a feature that is observed for all values of ϕ and η, even close to the cluster state. Similar observations have been made in Ref. [14].

Figure 7(b) shows the behavior of the exponent α. This behavior is very different from the case of uniform heating. For uniform heating α has the same value over the entire observed range of velocities. For boundary heating, on the other hand, α has a constant value α_1 over the low-velocity range but crosses over to different value α_2 when above a critical velocity v_c. For all rings the distribution for smaller velocities is close to Gaussian with $\alpha_1\approx 1.8$. For the inner three rings the distribution for velocities higher than v_c is well described by a single exponent $\alpha_2<1.5$. For the outer rings this behavior is more complicated.

In Fig. 8 we show the effect of a change in ϕ and η on the shape of the velocity distributions. Here we focus on the

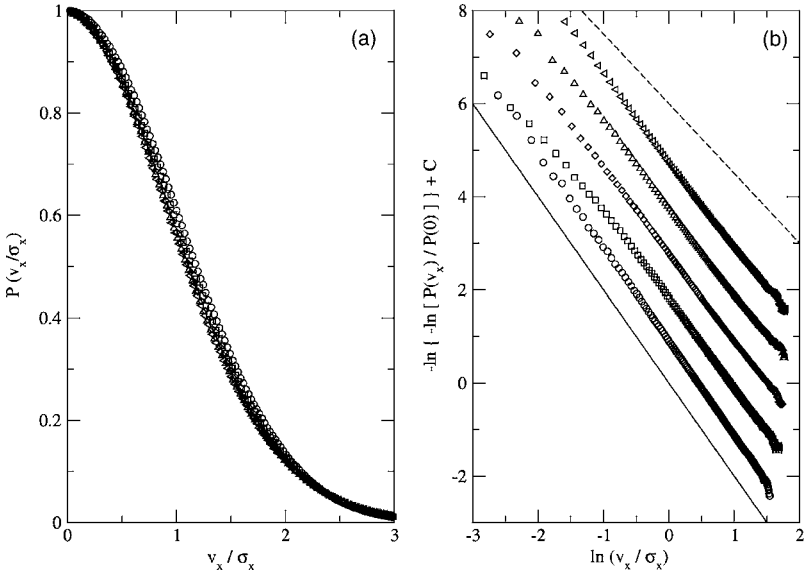

FIG. 3. Uniform heating. (a) $P(v_x/\sigma_x)$. (b) $-\ln\{-\ln[P(v_x/\sigma_x)]\}$ vs $\ln(v_x/\sigma_x)$. Data for both figures are taken for $N=350$ and for $\phi=0.02$ and $\eta=0.8$ (○), 0.6 (□), 0.4 (◇), 0.2 (△), and 0.1 (◁). A Gaussian is shown as a solid line with slope −2 and the distribution obtained by Rouyer and Menon is shown as the dashed line with slope −1.5. The velocity distributions are shifted by a constant amount C for clearity.

velocity distribution as measured in the ring with $0.4<r\leqslant 0.6$. This has the advantage of good statistics, but for values of ϕ and η close to a cluster, we might see effects due to the density gradient in the gas. As shown in Fig. 8(a) the exponent $\alpha_1=1.8$ except for $\eta=0.4$, where $\alpha_1=1.6$. For $\eta=0.9$ there is no crossover in the observed range of velocities. In the other distributions one does observe a crossover and the point where it occurs shifts down to lower velocities as η is decreased. It is clear that the distribution for velocities above the crossover cannot be described by a single exponent. For low enough η, the distribution seems to approach a constant exponent for high velocities. This exponent decreases from $\alpha_2=1.3$ for $\eta=0.7$ to $\alpha_2=1.0$ for $\eta=0.4$. Velocity distributions with a similar dependence on η have been observed before in Refs. [5,19].

In Fig. 8(b) we examine the behavior of the velocity distributions as the area density is varied. Again, we find that for smallest velocities the distribution is close to Gaussian with $\alpha_1\approx 1.8$ for all ϕ. A crossover in exponent α is observed for every ϕ and the velocity at which the crossover occurs hardly shifts as ϕ is varied. The distributions approach a constant exponent for high velocities. This exponent goes down from $\alpha_2=1.5$ for $\phi=0.01$ to $\alpha_2=1.0$ for $\phi=0.05$. In general, the deviations from Gaussian become more pronounced as dissipation increases, i.e., as ϕ increases or as η decreases. When α_2 decreases it is increasingly difficult to describe the distribution with an single exponent α_2 for the highest velocities. It may well be that this regime, corresponding to the highest velocities in both our simulations and the recent experiments, is different from the *asymptotic* high-velocity tail predicted by kinetic theories [7].

To test whether the velocity distributions we find here are only observed for this specific driving mechanism of heating through a circular boundary, we constructed different systems that drive through boundaries in a different way. For instance, we constructed a box with periodic boundary conditions that includes a small circular region around the center. Within this circular region particles are uniformly driven but outside of the region they are not heated at all. For par-

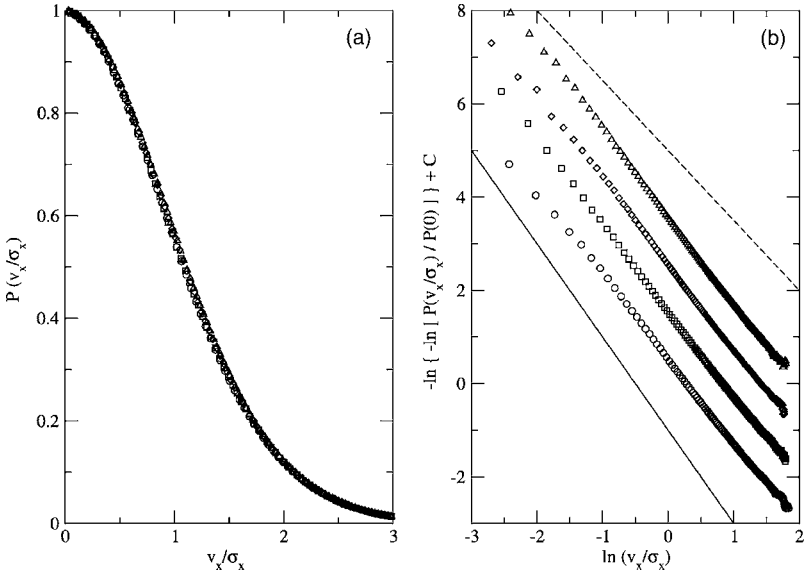

FIG. 4. Uniform heating. (a) $P(v_x/\sigma_x)$. (b) $-\ln\{-\ln[P(v_x/\sigma_x)]\}$ vs $\ln(v_x/\sigma_x)$. The dashed lines have slopes −2 and −1.5. Data for both figures are taken for $N=350$ and for $\eta=0.2$ and $\phi=0.1$ (○), 0.05 (□), 0.02 (◇), and 0.01 (△).

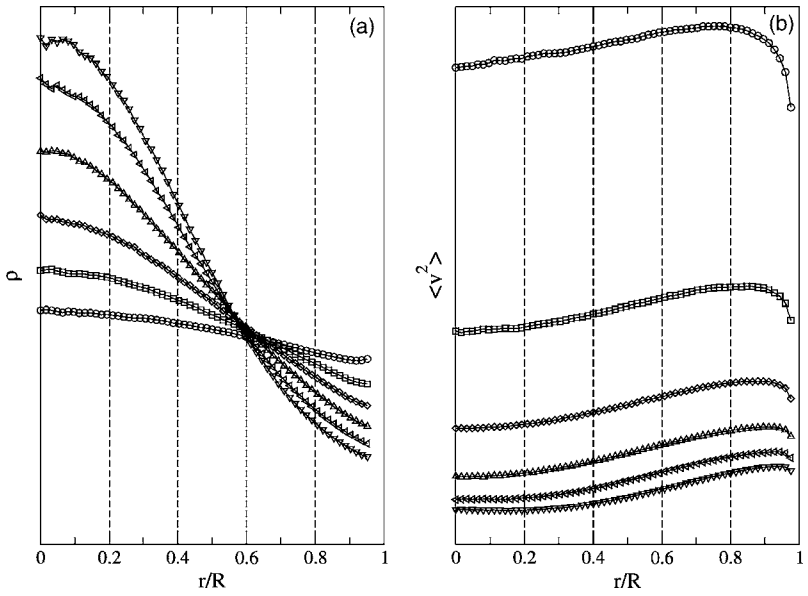

FIG. 5. Boundary heating. (a) The average number density ρ as a function of distance r to the center of the box. The container has radius R. Data taken for $N=350$, $\phi=0.02$, and $\eta=0.9$ (○), 0.8 (□), 0.7 (◇), 0.6 (△), 0.5 (◁), and 0.4 (▷). (b) The mean kinetic energy $\langle v^2 \rangle$ per particle as a function of r, for the same values of ϕ and η. The dashed lines indicate the concentric rings, within which the velocity distributions were separately calculated.

ticles within the circular region we observe velocity distributions that are Gaussian. On the other hand, for particles outside of the circular region we observe the same non-Gaussian velocity distributions as seen in the case of a circular boundary.

To test whether velocity distributions are sensitive to the precise way of heating at the boundary, we changed our heating algorithm so that when a particle hits the boundary, the angle of reflection is random and the magnitude of the new velocity is drawn from a Gaussian distribution. This has a minor effect on the distribution for the highest velocities, but leaves all major differences between uniform and boundary heating intact.

Finally, we studied the behavior of the velocity distribution for different particle numbers N. Figure 9(a) shows that, as N increases, the velocity distributions become more narrow for smaller velocities, but fall off less rapidly in high velocity regime. This is shown more clearly in Fig. 9(b). We find that the distribution for velocities larger than the crossover velocity is well described by a single exponent that decreases from $\alpha_2=1.7$ for $N=50$ to $\alpha=0.7$ for $N=1000$. The crossover shifts to lower velocity and becomes sharper as N is increased. Instead of approaching a limiting velocity distribution as N is increased, we find that the shape of the velocity distribution depends not only on η and ϕ, but also on N for all values of N we examined. This indicates that for boundary heating there is no thermodynamic limit. For uniform heating, on the other hand, the velocity distribution is largely insensitive to changes in N, because each particle individually is in contact with the heat bath. Even though the velocity distribution for boundary heating depends sensitively on η, ϕ, and N, we showed in Ref. [16] that the velocity distributions collapse onto each other for each η and $q=(N\phi)^{-1/2}$.

The most obvious difference between uniform and boundary heating is that in the first case heating takes place homogeneously throughout the box, whereas in the latter case energy is injected inhomogeneously at the boundaries. That this

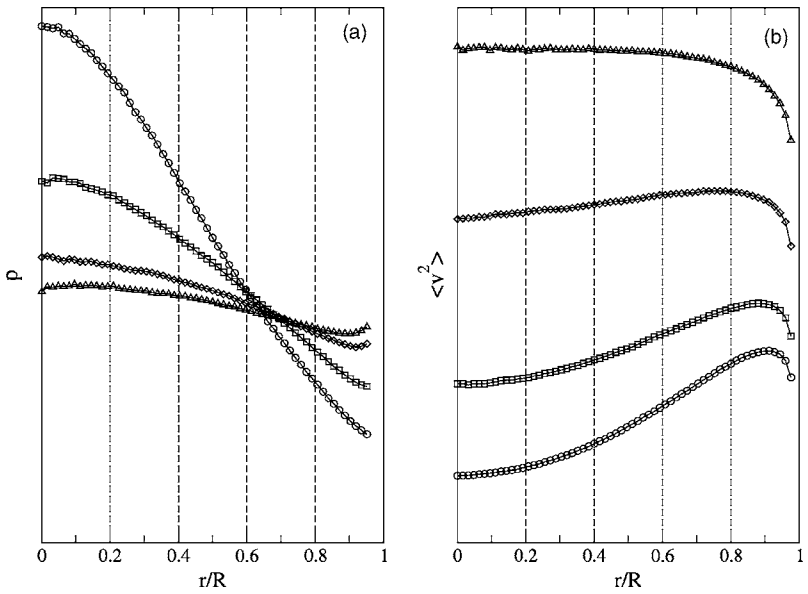

FIG. 6. Boundary heating. (a) The average number density ρ as a function of distance r to the center of the box. Data taken for $N=350$, $\eta=0.9$ and $\phi=0.1$ (○), 0.05 (□), 0.02 (◇), and 0.01 (△). (b) The mean kinetic energy $\langle v^2 \rangle$ per particle as a function of r, for the same values of ϕ and η. Note that even for the dilute case $\phi=0.01$ the mean kinetic energy profile is not constant, but drops at the boundary of the box. The profile only becomes constant after a certain distance into the container, which corresponds to the mean free path of particles leaving the boundary. This feature, together with the rise in density that we observe close to the boundary, has been described also in Ref. [19].

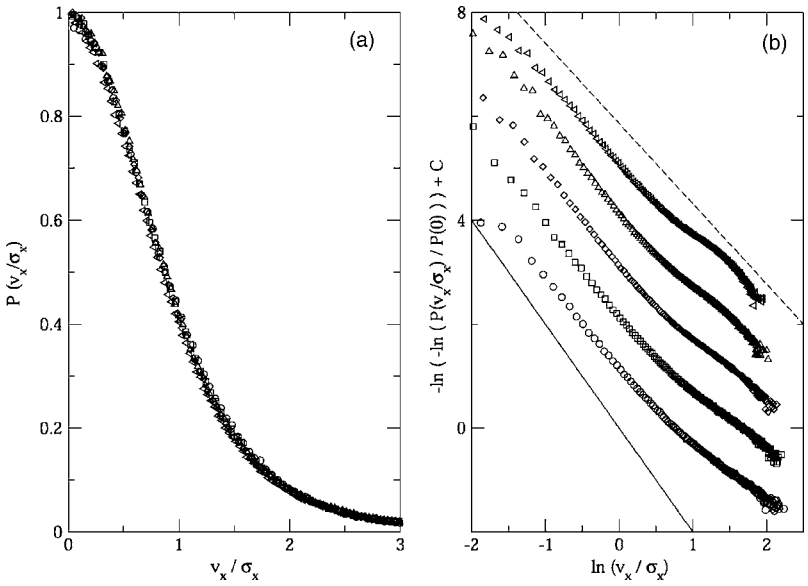

FIG. 7. Velocity distributions for boundary heating calculated separately within the concentric rings shown in Figs. 5 and 6, i.e., for $0<r\leqslant 0.2$ (○), $0.2<r\leqslant 0.4$ (□), $0.4<r\leqslant 0.6$ (◇), $0.6<r\leqslant 0.8$ (△) and $0.8<r\leqslant 1$ (◁), where r is distance to the center. Data were taken for $N=350$, $\phi=0.05$, and $\eta=0.8$. (a) $P(v/\sigma_x)$. (b) $-\ln\{-\ln[P(v_x/\sigma_x)]\}$ vs $\ln(v_x/\sigma_x)$. The local slope corresponds directly to the local exponent α.

is not the cause for the difference in velocity distributions, we show by using a different heating mechanisms that is spatially homogenous but where the ratio q can be adjusted. With this heating mechanism, described in Ref. [4], we can reproduce the entire family of distributions as observed for boundary heating. In this case, for every time step Δt we select at random two particles and add to these particles a random but opposite velocity to conserve the total momentum. On average heating is spatially homogeneous and in the limit of small Δt this heating mechanism approaches uniform heating. When Δt is small, many heatings occur for every collision whereas for large Δt, particles collide many times before being heated. By increasing Δt, the parameter q is decreased.

The effect of changing Δt is shown in Fig. 10. Here, we show the velocity distribution for $N=350$, $\phi=0.02$, and $\eta=0.4$. The gas is heated using the two-point heating algorithm described above, while we vary the time between heatings, Δt. For $\Delta t=0.01$ the distribution has a exponent $\alpha=1.7$ that is approximately constant over the observed range. When Δt is reduced a clear crossover develops. The behavior of the velocity distribution for velocities higher than the crossover velocity is more complicated than in boundary heating. There is also a sharp kink at the high-velocity end that we have been unable to explain so far. For small Δt, the velocity distribution is Gaussian over the entire range of velocities. For larger Δt, the resulting velocity distribution is reminiscent of the distributions seen for boundary heating, where a crossover in the exponent occurred for similar values of η. This reinforces the idea in Ref. [16] that uniform heating and boundary heating describe different limits of the same granular gas, for $q\gg 1$ and $q\sim 1$, respectively.

V. A SIMPLE MODEL WITHOUT SPATIAL DEGREES OF FREEDOM

In Ref. [16] we studied a simple model of an inelastic gas without spatial degrees of freedom. With this model, we are

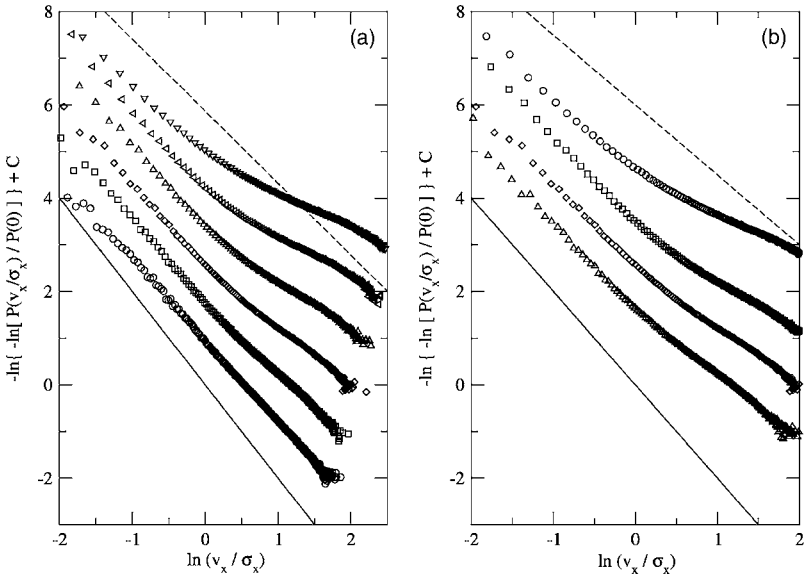

FIG. 8. Boundary heating. (a) $-\ln\{-\ln[P(v_x/\sigma_x)]\}$ vs $\ln(v_x/\sigma_x)$ for $N=350$, $\phi=0.02$ and $\eta=0.9$ (○), 0.8 (□), 0.7 (◇), 0.6 (△), 0.5 (◁), and 0.4 (▽). (b) $-\ln\{-\ln[P(v_x/\sigma_x)]\}$ vs $\ln(v_x/\sigma_x)$ for $N=350$, $\eta=0.7$ and $\phi=0.01$ (○), 0.02 (□), 0.03 (◇), and 0.05 (△).

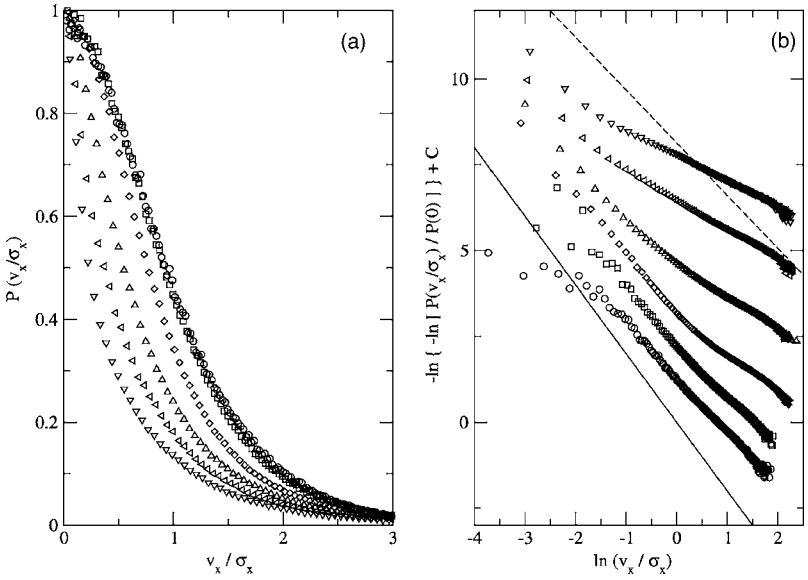

FIG. 9. Boundary heating. (a) $P(v_x/\sigma_x)$ for different values of N. (b) $-\ln\{-\ln[P(v_x/\sigma_x)]\}$ vs $\ln(v_x/\sigma_x)$. Data are taken for $\phi=0.05$, $\eta=0.8$ and $N=50$ (○), 100 (□), 200 (◇), 500 (△), 700 (◁), and 1000 (▽).

able to reproduce the velocity distributions observed in uniform and boundary heating by adjusting the parameter q. This shows that spatial correlations or inhomogeneities due to the presence of driving boundaries play a minor role in explaining the non-Gaussian velocity distributions observed in experiments. Even though kinetic theories have established that certain specific non-Gaussian velocity tails arise in the absence of spatial correlations [7–9], it has remained an open question whether the entire family of non-Gaussian velocity distributions observed in experiments can be explained without spatial correlations [20]. In this section, we explore the behavior of this model in more detail by systematically varying the two parameters of the model, η and q.

In our model, every time step we select at random C pairs of particles i and j and let them collide. At the same time we randomly select H particles k and heat those by adding a random amount to their velocity. We model collisions as follows: Eq. (1) can be cast into the following form:

$$\mathbf{v}_i' = \mathbf{v}_i - \frac{1+\eta}{2}\begin{pmatrix} \cos^2\theta & \sin\theta\cos\theta \\ \sin\theta\cos\theta & \sin^2\theta \end{pmatrix}(\mathbf{v}_i - \mathbf{v}_j), \quad (4)$$

where $\mathbf{v}_i$ and $\mathbf{v}_i$ are the velocities of particles i and j, η is the coefficient of restitution and θ is the angle between the separation vector $\mathbf{r}_{ij}$ and a reference axis. Collisions in our model occur by selecting at random particles i and j and an uniformly distributed impact parameter $-2R<b<2R$. We then use the above collision rule with $\theta=\arcsin(b/2R)+\arccos(\mathbf{v}\cdot\hat{\mathbf{s}}/v)$, where $\mathbf{v}=(\mathbf{v}_j-\mathbf{v}_i)/2$ is the velocity in the center-of-mass frame and $\hat{\mathbf{s}}$ is a unit vector along the reference axis. We discard values of θ corresponding to $(\mathbf{v}_j-\mathbf{v}_i)\cdot\mathbf{r}_{ij}<0$ as these represent unphysical collisions. We heat the particles k by adding a random amount of velocity according to Eq. (2). To prevent the velocities from running away, we subtract the center-of-mass velocity after heating. In a single time step, $N_H=H$ particles are heated and N_C

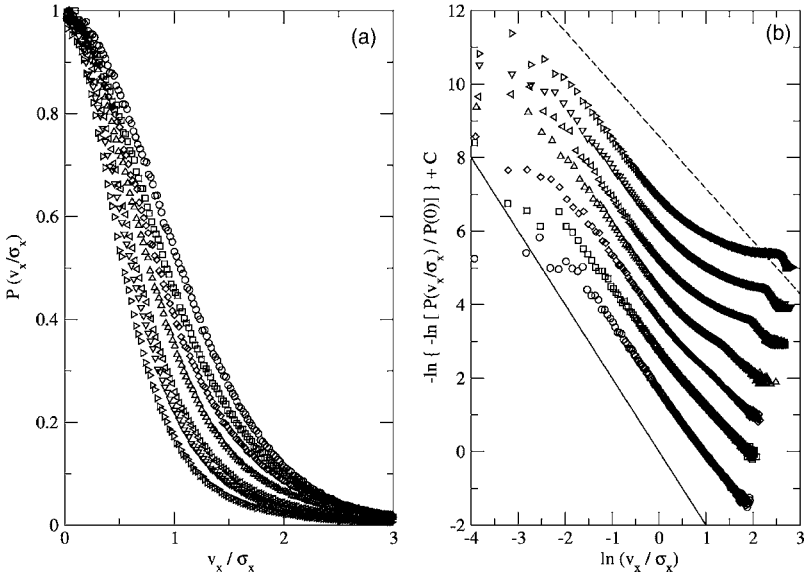

FIG. 10. Two-point heating. (a) $P(v_x/\sigma_x)$ for different values of Δt. (b) $-\ln\{-\ln[P(v_x/\sigma_x)]\}$ vs $\ln(v_x/\sigma_x)$. Data are taken for $N=350$, $\phi=0.02$, $\eta=0.4$, and $\Delta t=0.01$ (○), 0.03 (□), 0.05 (◇), 0.10 (△), 0.30 (◁), 0.50 (▽) and 1.00 (▷).

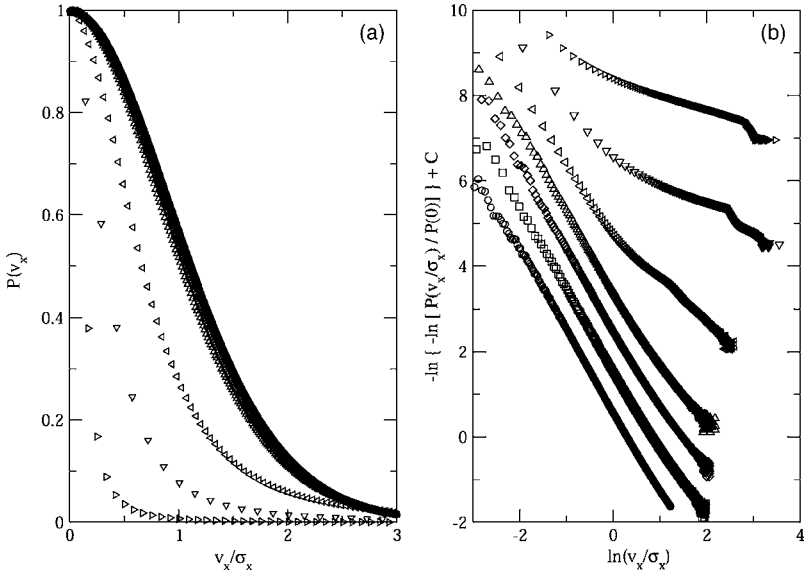

FIG. 11. Velocity distribution for the simple model with $N=500$ and $\eta=0.4$. (a) $P(v_x/\sigma_x)$. (b) $-\ln\{-\ln[P(v_x/\sigma_x)]\}$ vs $\ln(v_x/\sigma_x)$. Data are for different values of $q=H/2C$: $q=50$ (○), $q=5$ (□), $q=1$ (△), $q=0.5$ (△), $q=0.05$ (◁), $q=5\times10^{-3}$ (▽), and $q=5\times10^{-4}$ (▷).

$=2C$ particles collide. As a consequence, $q=H/(2C)$. This model is similar to the inelastic Maxwell model with white-noise forcing [8], but here, in addition, we can explicitly adjust the heating and collision independently, allowing us to study the behavior as a function of q. As such it is based upon the work of Ulam [21], but including dissipation.

In Fig. 11 we plotted the result for an inelastic gas with $\eta=0.4$. We varied the number of heatings and the number of collisions in a single time step from $H=100$ and $C=1$ to $H=1$ and $C=1000$. As q is lowered, the velocity distributions develop a crossover and for $q\ll1$ the distributions are strongly non-Gaussian, similar to the velocity distributions obtained for $\Delta t\gg1$ in two-point heating. In Fig. 12 we keep $q=0.025$ fixed and vary η. We see that the crossover point shifts to lower velocities as η is lowered.

Whereas we showed in Ref. [16] that this model yields velocity distributions comparable to uniform and boundary heating for similar values of q, here it is clear that the model also qualitatively reproduces the family of distributions observed for the simulations. The transition in Fig. 11 as q is increased compares well to the same transition in Fig. 10, where Δt is decreased. Also, the crossover that develops in Fig. 8 as η is increased is similar to those seen in Fig. 12. This confirms that the velocity distributions are non-Gaussian not because of spatial correlations. Rather, it is the flow of energy through the system, mediated by the inelastic collisions, that determines the shape of the velocity distribution.

VI. RELATION TO EXPERIMENTS

Unfortunately, experimental results for velocity distributions have remained ambiguous. Different setups and driving mechanisms usually give different velocity distributions. The distribution with a universal exponent of $\alpha=1.5$ was obtained by Rouyer and Menon for a setup where particles were confined between two vertical plates and driven in the vertical direction. However, for a different setup, where particles on a horizontal plate were driven in the vertical direction, Olafsen and Urbach [17] found crossovers from expo-

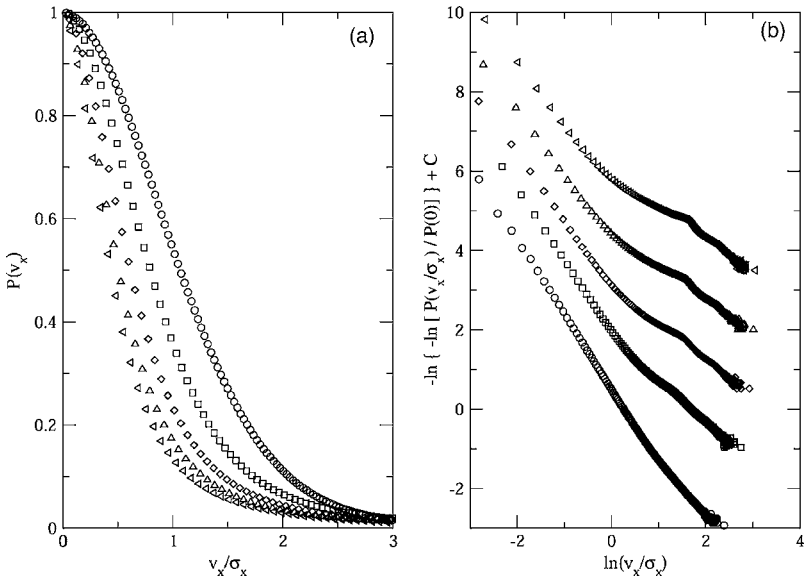

FIG. 12. Velocity distribution for the simple model with $N=500$ and $q=0.025$. (a) $P(v_x/\sigma_x)$. (b) $-\ln\{-\ln[P(v_x/\sigma_x)]\}$ vs $\ln(v_x/\sigma_x)$. Data are for $\eta=0.9$ (○), 0.7 (□), 0.5 (◇), 0.3 (△), and 0.1 (◁).

nential to Gaussian distributions when changing the driving of the particles. Blair and Kudrolli [11] used a setup where particles move along an inclined plane. Friction with the plane during collisions reduced the coefficient of restitution to $\eta \approx 0.5$, much lower than the coefficients of restitution usually reached in other setups. They found the distribution with exponent $\alpha = 1.5$ only in the very dilute case. Otherwise, the distributions deviated strongly from both Gaussian and the distribution obtained by Rouyer and Menon. This different behavior of the velocity distribution from experiment to experiment has yet remained unexplained, although friction between particles and the sidewalls may account for it to some extent [22].

Because of the absence of gravity and friction in our simulations, it is not possible to do a direct comparison between our simulation and experiments. In the experiment of Rouyer and Menon the driving is through the boundary, but there are some significant differences between their heating mechanism and the one we use in simulations with boundary heating. Due to gravity and the geometry of the setup the injection of energy in the experiment of Rouyer and Menon is mainly in the vertical direction. This energy is transferred into the horizontal direction by collisions between particles. Another difference is that in the experiment the frequency of driving is relatively low. Because of this the dynamics of the gas close to the driving boundary is strongly dependent on the phase of the driving cycle. In fact, it has been shown in simulation that for a system similar to the experiment by Rouyer and Menon, a shock wave propagates up through the gas [23]. At a certain distance from the boundary the time dependence has decayed and the gas enters a steady state. It is in this steady state that the velocity distributions are measured.

It is not yet established how this time dependence and the occurrence of a shock wave influences the velocity distributions in the steady state. *A priori* it is not clear if it is possible to compare velocity distributions in systems with a strong time dependence, like the experiments, with those that have no time dependence, as is the case in our simulations. There are, however, reasons to assume this is possible. The velocity distributions in the experiment of Rouyer and Menon are measured only in the direction orthogonal to the driving direction. Simulations [23] show that the effect of the shock in the direction orthogonal to the shock is usually relatively weak and decay rapidly in height. In the steady state, influence of the shock is absent in the orthogonal direction, even while it still may be apparent in the direction perpendicular to the driving direction. So, if we only look at velocity distributions in the orthogonal direction and in the steady state, a comparison between the experiment and our simulations is justified.

It is also not clear how in this experiment the dynamics of the gas shape the velocity distribution and whether it is controlled by the parameter q. We speculate that in the steady state the system behaves in fact like a one-dimensional inelastic gas. Fast upward moving particles inject energy in the orthogonal direction when colliding with particles in the steady state, effectively functioning as a heat source. In this picture the mean number of collisions between fast upwards moving particles and particles in the steady state would be N_H, the average number of heatings, and collisions between the particles in the steady state mutually would be N_C, the average number of collisions. One way of changing the shape of the velocity distribution would be to change the fraction of particles in the steady state. More particles in the steady state would lower N_H and increase N_C leading to more non-Gaussian velocity distributions.

The above considerations not only apply to the experiment of Rouyer and Menon but to most of the other experiments as well. In the experiments of Blair and Kudrolli and those of Olafsen and Urbach velocity distributions are measured orthogonal to the driving direction. In both cases it is not so much the collisions with the bottom plate that drive the gas in the orthogonal directions, but mainly off-angle collisions between fast upward moving particles with particles that have low velocities in the orthogonal directions. It is in these experiments rather than those of Rouyer and Menon that we find a similar dependence on η and q as described in this paper.

In the setup of Olafsen and Urbach [17] velocity distributions go from non-Gaussian to Gaussian when a rough plate is used instead of a flat plate. On a flat plate, energy is injected only in the in-plane directions by off-angle collisions between neighboring particles. With a rough plate, energy is injected directly into the directions parallel to the plate every time a particle collides with the plate, effectively increasing the number of heatings over collisions. Baxter and Olafsen [24] observe the same behavior in a system where a layer of heavy particles is inserted between the other layer of particles and a flat bottom plate. Particles from the upper layer have off-angle collisions with the layer of heavy particles, injecting energy in the in-plane directions every cycle. Particles in the upper layer show Gaussian velocity distributions, whereas particles in the lower layer have non-Gaussian velocity distributions.

The clearest sign of a potential role of q is seen in an experiment by Blair and Kudrollli [11]. Here the number of collisions is increased by adding more particles. As a result, their velocity distributions develop the same crossover that we see both in our simulations and models. The reason why these transitions are not visible in the experiment by Rouyer and Menon as they increase the number of particles, is likely that in the first case the effective coefficient of restitution is much lower, $\eta \approx 0.5$, due to friction with the inclined plane. These observations have recently been reproduced in simulation [25].

Again, one of the main problems considering the velocity distributions in granular gases is that different setups and experiments usually find different velocity distributions. As we have shown in this section, this variation in velocity distributions could be accounted for largely by changes in the parameter q among the different setups and experimental conditions. In this way, our finding of the controlling parameter q could ultimately explain these seemingly inconsistent results.

VII. CONCLUSION

We compared the velocity distributions of a granular gas that was driven by uniform heating and by heating through

the boundary. Both in theory and simulation studies, it is often implicitly assumed that far from the boundary the dynamics of granular gases is well described by uniform heating. Here and in Ref. [16], we find that there are clear qualitative differences. When driven through the boundary, for instance, the gas can form coexisting "cool" liquidlike clusters surrounded by a "hot" gaseous state for certain values of ϕ and η. Such clusters do not occur in our simulations with uniform heating. For increasing dissipation, these cluster grow in size and ultimately exhibit crystalline order.

The difference between uniform heating and boundary heating also extends to the velocity distributions. In both cases, we studied the dynamics of the granular gases while systematically varying all relevant parameters. For uniform heating, we confirmed that the distribution was close to Gaussian for a wide range of the coefficient of restitution η, area fraction ϕ, and particle number N. When heating through the boundary, we found that the granular gas developed spatial gradients in density and mean kinetic energy, with density peaking in the center and mean kinetic energy at the boundary. Surprisingly, the velocity distribution are relatively insensitive to the precise position in these gradients. When normalized by the mean kinetic energy, the velocity distributions collapse on each other, consistent with previously reported results [10,14]. For boundary heating, the velocity distribution is often non-Gaussian, with the precise shape depending sensitively on η, ϕ, and N. Only for dilute systems of almost elastic particles do we find the Gaussian distribution that is always observed for uniform heating.

In Ref. [16] we proposed that the difference between uniform and boundary heating is mainly in the control parameter q, the ratio between the average number of heatings, and the average number of collisions in the gas. To test whether this difference is not due to the imhomogeneity of energy injection, we studied the velocity distributions in a system where the energy injection is spatially homogeneous but where q can be varied easily. In this system, we directly observe the transition from Gaussian to strongly non-Gaussian velocity distributions as we decrease q. This supports our idea, that uniform heating and boundary heating represent different limits of the same inelastic gas, but for $q \gg 1$ and $q \lesssim 1$, respectively.

Finally, a simple model of a driven, inelastic gas without spatial degrees of freedom reproduces the entire family of velocity distributions we find in simulation, as we vary η and q. This means that the velocity distributions are non-Gaussian not because of spatial correlations. Rather, it is the cascade of energy from a few high-energy particles to the slow-moving bulk of the gas that is the key determinant of the non-Gaussian velocity distributions. These observations should aid in the construction of a kinetic theory of dissipative gases and help explain the sometimes confusing results of recent experiments.

We thank L. P. Kadanoff, N. Menon, A. Kudrolli and D. Blair for useful conversations. This work is supported in part by the National Science Foundation under Grant No. PHY99-07949.

[1] S. McNamara and W. R. Young, Phys. Rev. E **50**, R28 (1994).
[2] T. Zhou and L. P. Kadanoff, Phys. Rev. E **54**, 623 (1996).
[3] D. R. M. Williams and F. C. MacKintosh, Phys. Rev. E **54**, R9 (1996).
[4] S. J. Moon, M. D. Shattuck, and J. B. Swift, Phys. Rev. E **64**, 031303 (2001).
[5] A. Barrat, T. Biben, Z. Racz, E. Trizac, and F. van Wijland, J. Phys. A **35**, 463 (2002).
[6] I. Pagonabarraga, E. Trizac, T. P. C. van Noije, and M. H. Ernst, Phys. Rev. E **65**, 011303 (2002).
[7] T. P. C. van Noije and M. H. Ernst, Granular Matter **1**, 57 (1998).
[8] M. H. Ernst and R. Brito, Phys. Rev. E **65**, 040301(R) (2002).
[9] M. H. Ernst and R. Brito, in *Granular Gas Dynamics*, edited by T. Poeschel and N. Brilliantov Lecture Notes in Physics Vol. LNP 624, (Springer-Verlag, Berlin, 2003); eprint cond-mat/0304608 (unpublished).
[10] F. Rouyer and N. Menon, Phys. Rev. Lett. **85**, 3676 (2000).
[11] A. Kudrolli and J. Henry, Phys. Rev. E **62**, R1489 (2000); A. Samadani and A. Kudrolli, *ibid.* **64**, 051301 (2001).
[12] W. Losert, D. G. W. Cooper, J. Delour, A. Kudrolli, and J. P. Gollub, Chaos **9**, 682 (1999).
[13] S. Luding, E. Clément, A. Blumen, J. Rajchenbach, and J. Duran, Phys. Rev. E **49**, 1634 (1994).
[14] A. Barrat and E. Trizac, Phys. Rev. E **66**, 051303 (2002).
[15] Y. Du, H. Li, and L. P. Kadanoff, Phys. Rev. Lett. **74**, 1268 (1995).
[16] J. S. van Zon and F. C. MacKintosh, Phys. Rev. Lett. **93**, 038001 (2004).
[17] J. S. Olafsen and J. S. Urbach, Phys. Rev. E **60**, R2468 (1999); **81**, 4369 (1998); A. Prevost, D. A. Egolf, and J. S. Urbach, *ibid.* **89**, 084301 (2002).
[18] A. Barrat and E. Trizac, Eur. J. Phys. **11**, 99 (2003).
[19] O. Herbst, P. Müller, M. Otto, and A. Zippelius, Phys. Rev. E **70**, 051313 (2003).
[20] A. Puglisi, V. Loreto, U. M. Marconi, A. Petri, and A. Vulpiani, Phys. Rev. Lett. **81**, 3848 (1998).
[21] S. Ulam, Adv. Appl. Math. **1**, 7 (1980).
[22] J. S. van Zon, J. Kreft, D. I. Goldman, D. Miracle, J. B. Swift, and H. L. Swinney, Phys. Rev. E **70**, 040301(R) (2004).
[23] J. Bougie, Sung Joon Moon, J. B. Swift, and H. L. Swinney, Phys. Rev. E **66**, 051301 (2002).
[24] G. W. Baxter and J. S. Olafsen, Nature (London) **425**, 680 (2003).
[25] D. Paolotti, C. Cattuto, U. Marini Bettolo Marconi, and A. Puglisi, Granular Matter **5**, 75 (2003).